Acoustically derived sediment fluxes: an acoustic-index to channel-average concentration approach

Dan Haught, Hydrologist, United State Geological Survey, California Water Science Center, Sacramento, CA, USA, Daniel.haught@gmail.com
Jeremy Venditti, Professor, Simon Fraser University, Burnaby, BC, Canada, jeremy_venditti@sfu.ca

Introduction

Knowledge of sediment flux in rivers is required for the management of navigable waters and reservoir maintenance. It is also critical to the understanding of aquatic habitat quality and morphodynamics of rivers and their deltas. Suspended sediment flux can be divided into material typically found in the bed, composed of sand-sized particles, and washload, composed of finer silt and clay-sized particles. The former is responsible for channel and bed morphology while the latter builds floodplains, deltas, and tidal flats. Washload is also important in the prediction of the transport and fate of pollutants that adhere to the finer suspended particles. Yet the prediction of washload remains difficult because supply generally determines transport rates, not hydraulics, like in the case of suspended bed material. The difficulty in prediction, along with the importance in higher resolution estimates, has led scientists and engineers to investigate acoustic-based suspended sediment monitoring programs.

Theoretically, the acoustic signal should respond to suspended sediments as a function of particle size, shape, mineralogy, and the number of particles in suspension. Therefore, back-calculating the acoustic signal should produce a reliable estimate of suspend sediment concentration, when minerology, shape, and size can be assumed constant. Clearly the latter is less likely, while the former two change over longer periods. Flammer (1962) shows how the backscatter of the signal is related to coarser suspended sediment such as silts and sands, while the attenuation of the signal with respect to distance away from the transducer is related to finer silts and clays. Additionally, many applications of this theory have related total suspended load to that of the backscatter in a more empirical fashion. Below, we examine these methods in order to derive a channel average concentration and flux.

Though a multitude of acoustic applications have been implemented, a recent approach has been to utilize horizontally projected Acoustic Doppler Current Profilers (H-ADCP) mounted to a stationary structure, such as a pier. This type of application works well in cases where the channel width is close to the range of the H-ADCP or the hydraulics maintain a well-mixed system. In large rivers, where H-ADCPs applied range is much smaller than the channel cross-section, correlation between the acoustically derived concentration and channel-average concentration is needed.

Methods

Discharge and Sediment Measurements:

We use a 600 kHz H-ADCPs to estimate suspended sediment concentration (SSC) and discharge, which provides an SSC flux. The H-ADCP was mounted to a dock at Mission, BC

Canada, in the Fraser River at a fixed elevation (-2.2 m amsl), which roughly covers the top 0.3 to 0.6 of depth depending on flow. The ADCP ensonifies a beam perpendicular to the flow and extends to approximately 60 m, while the total channel width at the site is 550 m. Physical sediment samples were collected within the acoustic ensonified volume as well as velocity profiles collected across five channel panels, to allow for the computation of channel-average SSC and flux. Samples were analyzed for SSC and gradation, allowing for calibration and the examination of the influence that changing gain-size has on the calibrations.

The index-velocity relation (Ruhl and Simpson, 2005) was systematically optimized by regressing measured velocity to the index velocity using the sum of squared residuals (SSR). This method utilizes a correlation between the velocity computed from the ADCP (index) to that of measured channel-average velocity. Using the index-velocity from the ADCPs, we varied the window size and location to identify the ideal fraction of ADCP cells to use in the index-velocity relation. We use the minimum SSR to select the optimized range of cells. Because stage data is a point measurement, we did not use a similar optimization for the stage-area analysis. The product of the channel-average velocity and the area is the channel-average discharge. Figure 1 shows the discharge for all three years of observation.

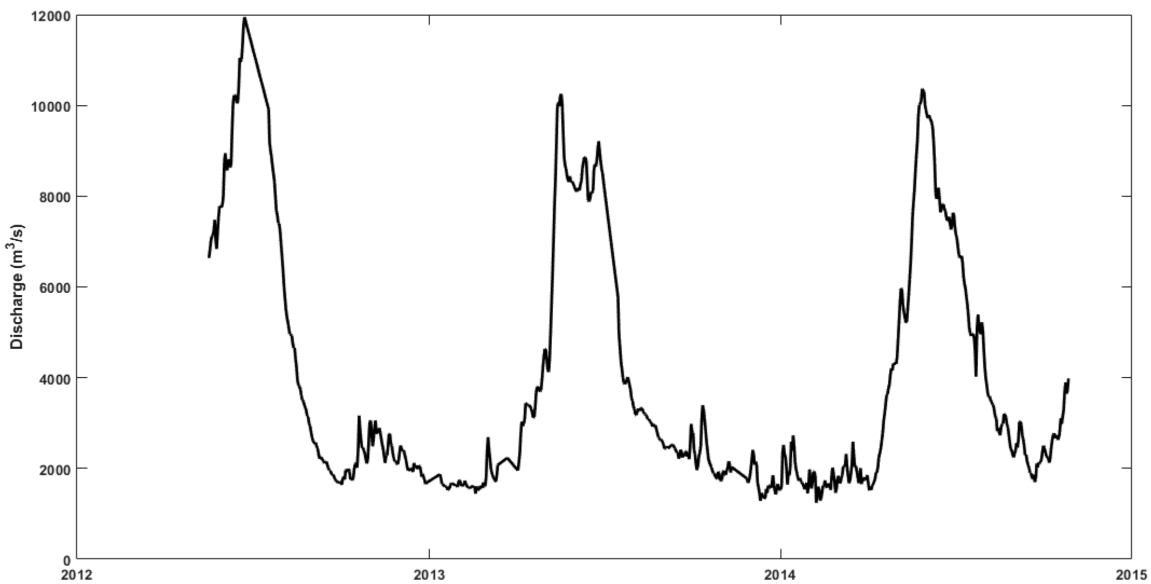

Figure 1. Discharge derived from the index-velocity method.

Acoustic Inversion:

We use a single-frequency acoustic inversion to correct the acoustic signal to account for sediment and fluid attenuation (Haught et al., 2017; Wright et al., 2010). The corrected acoustic signal is related semi-empirically to suspended sediment measurements within the ensonified volume. We calibrate total suspend sediment concentration (TSS) to fluid corrected backscatter (FCB), that is, the backscatter from the H-ADCP corrected to account for the attenuation due to fluid properties (primarily temperature). Sand concentrations are related to sediment corrected backscatter (SCB), which accounts for both fluid attenuation and sediment attenuation. Sediment attenuation is estimated from the slope of the regression between FCB and range (see Haught et al., 2017 and references therein). Because attenuation is derived from a regression with respect to space, it provides a single point in time and does not have a spatial context as does backscatter (Wright et al., 2010). The formal calibrations provide an estimate of TSS, sand

SSC, suspended bed material (SBM), and silt/clay SSC within the ensonified volume, but do not account for concentration variations across the channel.

To estimate channel-average concentration, similar to the index-velocity approach, we relate the index concentration within the ensonified volume to the channel-average concentration. Unlike the index-velocity method, an acoustic inversion must first be done to obtain H-ADCP derived concentrations. Regression relations are developed between the ensonified volume concentrations estimated by the H-ADCP and the measured channel average concentration for the respective suspended sediment fraction. We collected 4 to 6 sediment profiles per campaign with six discrete samples taken at a relative depth of 0.1, 0.2, 0.4, 0.6, 0.8, and 0.9 to compute channel average concentration. Similar to discharge, we optimized the relations by minimizing SSR, as described above.

Channel-average flux is computed from the channel-average discharge and the acoustically-derived channel-average concentration.

Results

Sediment Sampling:

Twenty-five sampling campaigns were carried-out in the Fraser River between 2012 and 2014. Sample concentrations ranged from 20-350 mg/L and were primarily composed of silt to fine sand (Figure 2).

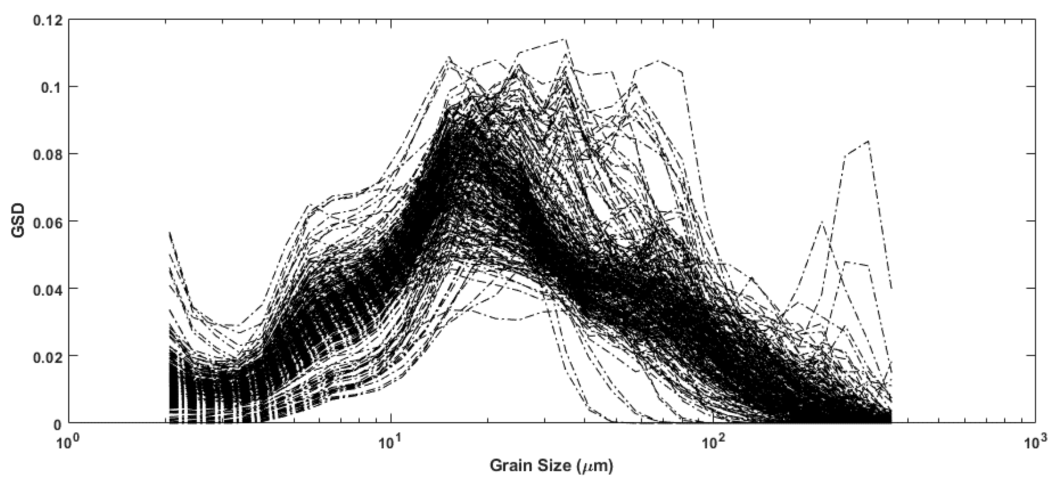

Figure 2. Gradation for samples collected in the ensonified volume and used to calibrate the H-ADCP.

Acoustic Calibration:

Acoustic inversions showed statistically significant calibrations between all SSC constituents. The coefficient of determination (R^2) was strong for Fine SSC, while the other constituents had weaker R^2 values. The TSS SSC calibration showed a large amount of scatter at lower SSC (Figure 3). Sand calibration shows less scatter than the SBM SSC (Figure 3 middle panel), while having stronger correlation (Table 1). Fine SSC provides the tightest grouping but shows some anomalies in the grouping (Figure 3 right panel). Because of the poor relation to SBM, we do not carry it forward in the development of a flux.

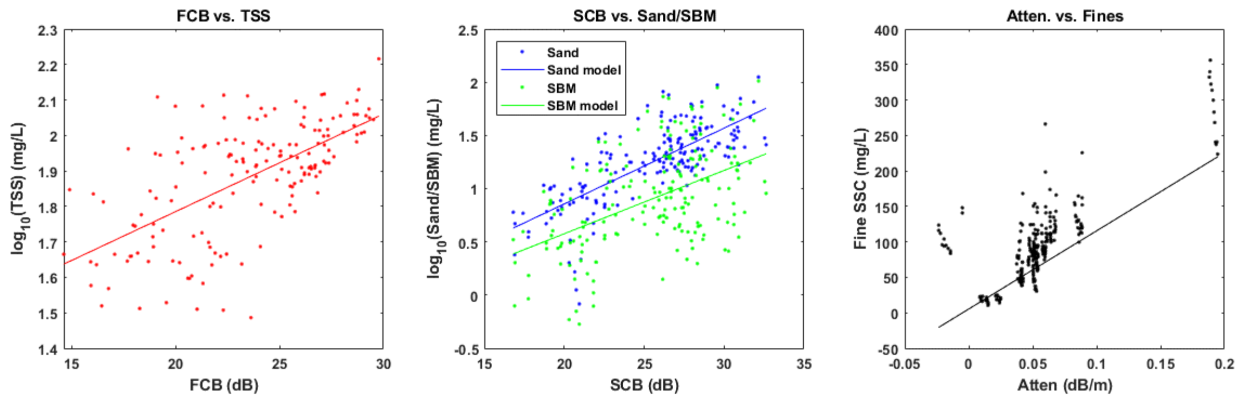

Figure 3. Calibrations between backscatter properties and SSC properties used to estimate ensonifed volume SSC.

Table 1. Statistics for the acoustic inversion calibrations

Calibration	R^2	Mean Square Error	p-value	SE of the slope
TSS	0.4	0.12	0	2.6e-3
Sand	0.57	0.06	0	4.6e-3
SBM	0.24	0.16	9.1e-13	7.7e-3
Fines	0.82	2.1e-4	0	2.2e-5

ADCP to Channel Average Relation:

To account for the limited range of the ADCP (60 m), we make a relation between what the ADCP derived SSC (from the calibrations above) and the measured channel average SSC. Relations between acoustically derived SSC and channel-average SSC had good correlation (Figure 4), allowing for estimates of continuous SSC and flux on a large river. In addition to deriving TSS acoustically, we also sum the acoustically derived sand SSC with fine SSC (Figure 4 right panel). The sum of the sand and fines produces a better result than acoustically derived TSS. Because of the better result from the sum of parts, we do not carry forward the assessment of TSS derived acoustically.

Figure 4 shows the correlations as scatter plots, while Table 2 provides the statistical assessment. The sand SSC relation provides the strongest correlation, while SBM does not capture the high concentrations as well as sand (Figure 4 center panel). Fine SSC shows good correlation, albeit possibly one outlier. We use these relations to develop channel average time series and a channel average flux.

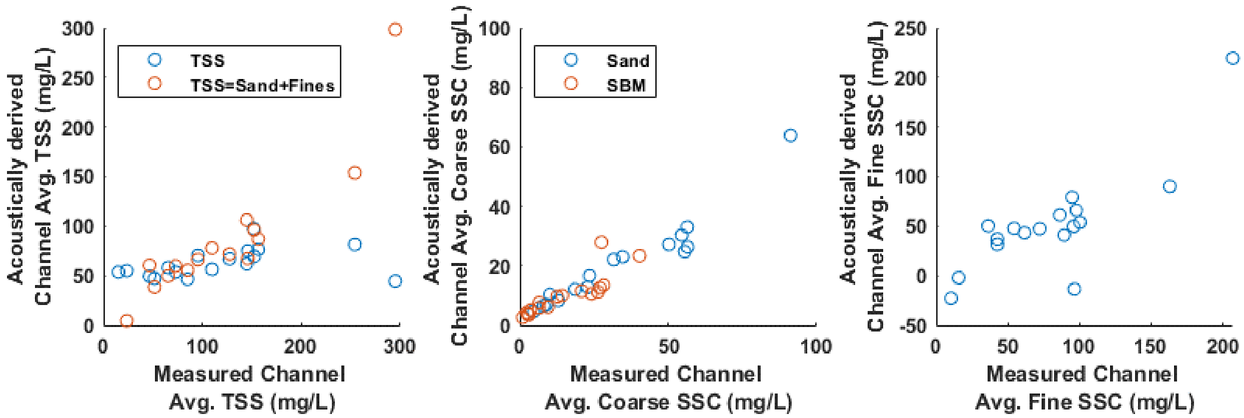

Figure 4. Relation between ensonified volume, acoustically derived, SSC and measured channel average SSC.

Table 2. Statistics for models developed between ensonified volume SSC and channel average SSC. Note SE is the standard error.

Calibration	R^2	Mean Squared Error	p-value	SE of the slope
TSS	0.13	190	0.15	0.05
TSS=Sand+Fines	0.82	858	2.8e-6	0.1
Sand	0.91	36	1.7e-9	0.05
Fines	0.68	946	4.8e-5	0.16

Figure 5 shows the time-series of daily average channel average flux for TSS derived from the sum of sand and fine SSC relation. We also show the discharge and the measured flux. Acoustically derived channel-average TSS tracks discharge well, albeit underestimating measured flux. Measurements from 2012 track the falling limb well but are of greater magnitude. Measurements from 2013 suggest that the acoustically-derived values missed a portion of the freshet possibly due to SSC gradation changes. Measurements from 2014 show that acoustically derived TSS captures the spring flush of fine sediments and the majority of the freshet. The falling limb tends to be underestimated.

Acoustically derived sand flux track measurements well in 2012 and 2014, but less well in 2013. Measurements in 2012 coincide with the falling limb well, but due to a lack of measurements throughout the freshet, it is difficult to predict how well it tracks peak sand fluxes. In 2013, acoustically derived sand fluxes clearly underestimate the freshet, but track the falling limb well, likely contributing to the poor results seen in TSS flux. Measurements in 2014 suggest that acoustically-derived values capture the freshet well but miss the early sand load.

Acoustically-derived fine flux compares well to measurements for all three sampling seasons. Measurements in 2013 are slightly underestimated, while in 2014 measurements track the acoustically-derived values well.

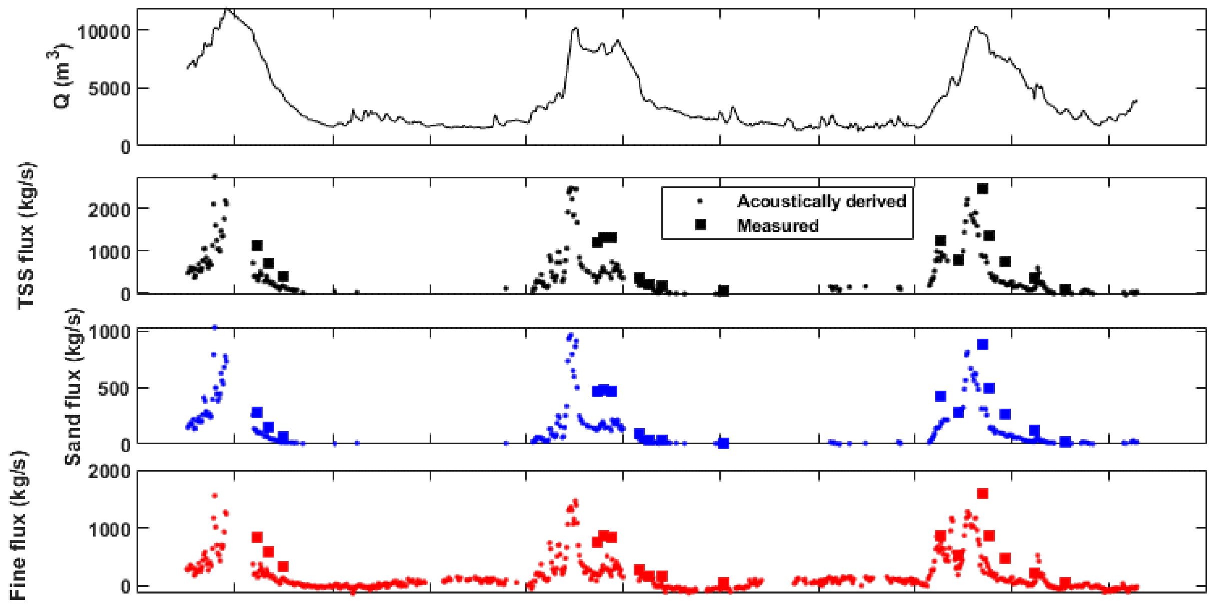

Figure 5. Time-series of flux data with measurements and discharge (top).

Figure 6 shows the relation between discharge and flux. Clearly a hysteretic effect is present. Relations show a clockwise hysteresis, suggesting that flux increases respond before peak discharge. Fine SSC flux shows the greatest hysteretic effect, likely due to an early spring first flush. Sand flux shows a tighter grouping. All three SSC constituents show a non-linear response.

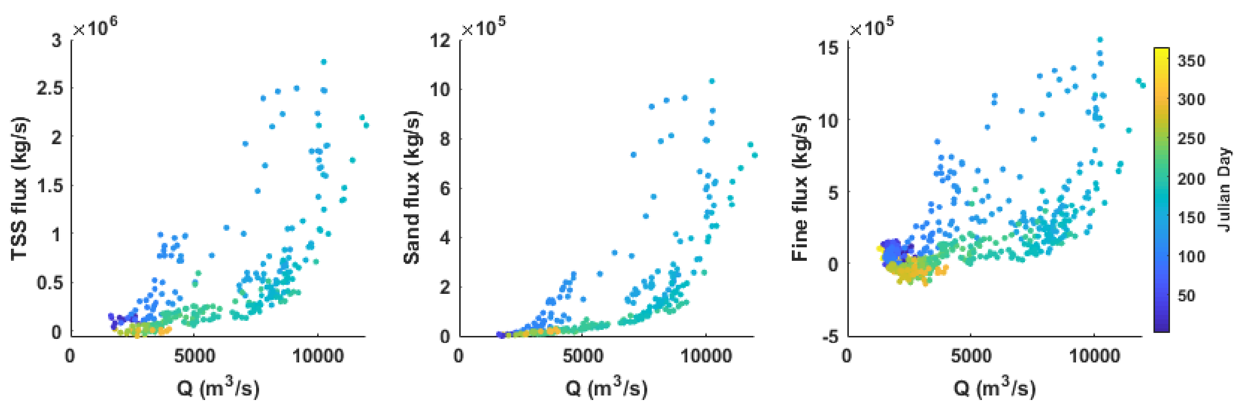

Figure 6. Hysteretic effect from the relation between Q and SSC flux.

Conclusion

Acoustically-derived SSC show that this method can capture the spatial and temporal dynamic that are a contemporary challenge to measure with physical sampling. We show how the direct relation of TSS to fluid corrected backscatter does not produce a strong calibration. This is likely due to the fact that sediment attenuation is not accounted for as it is with sediment corrected backscatter (which is related to sand). The sum of sand and fine sediment flux– both of which have a better response to acoustics– produces a better result, suggesting that the acoustic inversion is a valid estimate.

When relating the ADCP derived SSC to the channel average SSC, we provide a method for engineers, scientists and river managers to use in large systems where the instrument's range does not span the entire channel or at least a substantial portion of it. The linear relations show strong correlation and fall close to the line of unity. The fluxes from these relations track the flow and measurements well, while occasionally underestimating some measurements. Further measurements at the highest concentrations are needed to further assess these results and methodology.

This application clearly depicts the clockwise hysteretic nature of suspended sediment transport in the Fraser River. The clockwise hysteresis is a function of the spring first flush, where, as the flows rise, finer material stored near the bank is captured by the river and transported prior to the peak flow or sand transport. Once flows reach a threshold flow for sand transport, particularly fine sand, a pulse occurs prior to peak discharge. By the time the peak discharge is reached, there is a depletion of upstream sediment leading to a decline in SSC prior to the falling limb in dishcarge.

These estimates provide engineers and scientists the capability to better manage rivers with respect to dredging for navigable channels, along with the monitoring of sediment adhered pollutants and sediment budgeting.

References

Flammer, G. H., (1962), Ultrasonic measurement of suspended sediment, U.S. Geol. Surv., Bull. 1141-A. Govt. Printing Office, Washington, DC, 48 pp.

Haught, D., J. G. Venditti, and S. A. Wright (2017), Calculation of in situ acoustic sediment attenuation using off-the-shelf horizontal ADCPs in low concentration settings, Water Resour. Res., 53, doi:10.1002/2016WR019695.

Ruhl, C. A., and M. Simpson (2005), Computation of discharge using the index-velocity method in tidally affected areas, U.S. Geol. Surv. Sci.

Invest. Rep., 2005–5004, 41 p., U.S. Geol. Surv., Reston, Va.

Wright, S. A., D. T. Topping, and C. A. Williams (2010), Discriminating silt-and-clay from suspended-sand in rivers using side-looking acoustic

profilers, paper presented at the 2nd Joint Federal Interagency Sedimentation Conference, 27 Jun-1 Jul. Advisory Committee on Water Information, Subcommittee on Hydrology and Sedimentation, June, Las Vegas, Nev. [Available at http://acwi.gov/sos/pubs/2ndJFIC.]

Haught, D., J. G. Venditti, and S. A. Wright (2017), Calculation of in situ acoustic sediment attenuation using off-the-shelf horizontal ADCPs in low concentration settings, Water Resour. Res., 53, doi:10.1002/2016WR019695.